

Geoff Smith*, Angus Gentle, Matthew Arnold, and Michael Cortie

Nanophotonics-enabled smart windows, buildings and wearables

DOI: 10.1515/nanoph-2016-0014

Received September 9, 2015; accepted January 4, 2016

Abstract: Design and production of spectrally smart windows, walls, roofs and fabrics has a long history, which includes early examples of applied nanophotonics. Evolving nanoscience has a special role to play as it provides the means to improve the functionality of these everyday materials. Improvement in the quality of human experience in any location at any time of year is the goal. Energy savings, thermal and visual comfort indoors and outdoors, visual experience, air quality and better health are all made possible by materials, whose “smartness” is aimed at designed responses to environmental energy flows. The spectral and angle of incidence responses of these nanomaterials must thus take account of the spectral and directional aspects of solar energy and of atmospheric thermal radiation plus the visible and color sensitivity of the human eye. The structures required may use resonant absorption, multilayer stacks, optical anisotropy and scattering to achieve their functionality. These structures are, in turn, constructed out of particles, columns, ultrathin layers, voids, wires, pure and doped oxides, metals, polymers or transparent conductors (TCs). The need to cater for wavelengths stretching from 0.3 to 35 μm including ultraviolet-visible, near-infrared (IR) and thermal or Planck radiation, with a spectrally and directionally complex atmosphere, and both being dynamic, means that hierarchical and graded nanostructures often feature. Nature has evolved to deal with the same energy flows, so biomimicry is sometimes a useful guide.

1 Introduction

Scientific understanding of the optical and thermal response underpinning nanophotonic approaches to “smart” windows, buildings and wearables enables more efficient development, better production control and visual functionality tailored to personal choice [1]. Spectral and angular control of incoming and outgoing radiation across the solar and thermal radiation bands are usually


required in these applications. Nanostructures are excellent at achieving and tuning the sharp spectral transitions and angular responses desired. This sensitivity to nanostructure can, however, also introduce practical problems. Building products typically span large-to-moderate areas and to have significant impact on energy savings, personal comfort and city living conditions, they must be affordable. Thus, mass production and ease of installation without damage are required. Accurate reproduction of nanostructure over large areas thus means structural control at very small scales needs to be maintained across commodity-scale production. This is demanding given production may extend from hundreds to millions of square meters annually. Example problems we have observed on buildings include slight variations in nano- and microstructure in window coatings or special paints varying in color to an extent that the façade or roof of a major building looks odd.

Visual appearance, including color and glare if opaque, and tint if transparent or translucent, is crucial to widespread adoption. But in today’s world so is energy performance. The latter means solar reflectance (albedo) R_{sol} and thermal emittance values must be close to specifications across large areas. The value of R_{sol} is often now input into building computer codes such as EnergyPlus [2] and into many statutory standards (e.g. ANSI/NFRC 200-2014 [3]) covering energy or thermal performance. Thus, unless material design specifications are met, building occupants may find they are using much more energy than anticipated. Good initial performance is also not enough; today’s smart building materials must have durable outdoors optical performance [4]. Similarly, smart fabrics must be able to maintain functionality after the rigors of weaving and washing. This review will focus on the science of smart building materials and fabrics with proven or likely ability to meet these demanding practical criteria. A suitable lab-based optical response over a few cm^2 may be a good start, but scaling up, ease of application without damage and years of durability in normal use is essential for commercial success.

Interest in “smart” fabrics and flexible materials is growing [5, 6]. These are composite materials or structures that have been engineered to provide vastly improved

*Corresponding Author: Geoff Smith, Angus Gentle, Matthew

Arnold, Michael Cortie: E-mail: g.smith@uts.edu.au

 © 2016 Geoff Smith et al., published by De Gruyter Open.

This work is licensed under the Creative Commons Attribution-NonCommercial-NoDerivs 3.0 License.

functionality relative to their constituent materials, often with some “active” functionality that varies with stimulus. They have applications in clothing, in nanocosmetics, in buildings and in temporary outdoor structures including those used in agriculture and horticulture. Goals of wearable smart fabrics include thermal comfort, IR loss management, IR visibility at night and control of both solar and night sky-induced heat flow. Low or high emission just where thermal cameras sense is another emerging spectral need. Another optical goal is stunning appearance from new visual effects. Novel color, including spectral sharpness and striking changes with viewing angle, are a feature of visual responses enabled by nanostructures [7, 8]. In buildings, smart blinds and curtains can add to energy conservation, daylighting and viewing performance of windows and skylights [9]. They also add novel aesthetic appeal and facilitate dynamic control. Smart paints, polymers, fabrics and flexibles, retrofitted to existing buildings, will be integral to future energy saving, visual appeal and longevity. A flexible nanopolymeric material, with which the authors recently set a new benchmark in cool roof performance [10], is shown thermally and visually in Figure 1. Its nanophotonic principles have also been utilized for novel clothing [11].

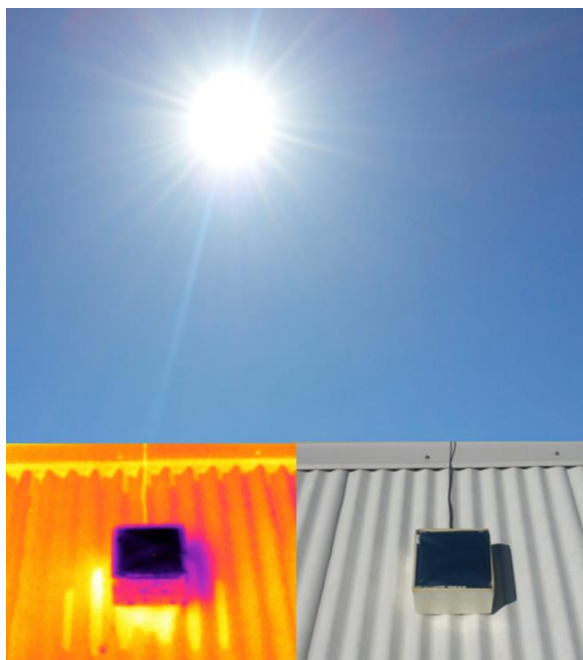


Fig. 1. A thermal image and a visual image of a supercool polymeric nanomaterial under the sky is shown. It is contrasted with a current commercial cool roof. The dark contrast of the coated box indicates that it is radiating significantly less energy than the hot roof on which it is located.

This review proceeds as follows. It starts with a thorough review of solar and atmospheric radiation as needed to assess material responses at any time, and over a typical year, when one or more surfaces are outdoors. The impact of humidity levels plus forced and natural convection must also be included in assessing such smart materials. These environment basics are introduced in Section 2. Section 3 combines these properties with the measured or theoretically modeled visible, near-IR and IR properties of building materials to determine their key solar, thermal and visual responses. The important role of angular response in cooling performance is included here. Goals for any smart multifunctionality, for example, in a window limiting solar heat gain while providing a clear view, good daylight and good thermal insulation, are then quantified. Section 4 deals with switchable smart materials in three classes, those that switch intrinsically to environmental change, those which are altered via applied forces in response to sensor signals and those which integrate the source of the force into their design. Generated charge or chemicals from conversion of some incident solar energy can be stored to be used later for switching. Section 5 analyses the smart response of a wide range of suitable nanomaterials. Section 6 examines approaches to nanofabrics and wearables with engineered spectral and thermal responses for various outdoor functionalities. Section 7 reviews the biomimicry of naturally occurring nanostructures where it has aided the development of materials with designed responses to environmental radiation flows, and Section 8 concludes.

2 Key environmental and human factors impacting smart material design

The primary goals in all this work are fulfilling various human needs, including: provision of clear vision into and out of structures, thermal comfort, high quality air, good health and enhanced lifestyle both indoors and outdoors. While we have managed to compensate technically indoors for most nonideal conditions, the energy, environmental and health costs in doing so are far too high. A new approach to the technology–environment interplay is needed. Harmonizing our living, working and leisure environments to external environmental energy flows will diminish such problems and shift to greater sustainability. In other words, how far can we go to make city life feel more “natural”? A key aspect of “natural” nanophotonics

is hierarchical nanostructures [12]. Such materials when reverse engineered into components, or imaged at several distinct magnifications, reveal multiple components each with a characteristic topology and scale, spatial arrangement and shape. The basic hierarchy in core-metal shell nanoparticles opened up opportunities for tuning of narrow plasmonic resonances unavailable in the metal itself. Nanoparticles embedded within a long fiber with a microscale cross-section, which are then twisted together into a macrofiber, is a more complex hierarchy. Two examples using columnar structures in our work are tapering of silicon columns, which leads to “black silicon” [13] and GLAD (glancing angle deposition) of high melting point materials, which form tilted nanocolumns whose spectral response is modulated by the hierarchy imposed by the way sets of columns line up in planes normal to the deposition plane [14]. Each smart material detailed in this review involves some structural hierarchy that enables better optical control over the very large bandwidth involved (0.3–35 μm) and for a full hemisphere of incidence directions. The angular and spectral response of smart building materials and across a wide energy band is integral to achieving this goal. The best solar thermal collectors are possible because a thin nanolayer can be made to absorb solar energy very strongly, but its scale makes it almost invisible to IR rays due to their micron wavelengths which then “see” the thick IR reflecting substrate so heat is not lost by radiation. This smart example is achieved by a basic layering hierarchy. Examples follow involving more complex layering hierarchies in which grading in multilayer thicknesses or particle fill factor across a wide range enables fine spectral and angular tuning of reflectance, absorptance and, if desired, transmittance. We need each surface to have designed responses which account for:

- Heating, daylighting and glare from solar energy radiation. A standard spectrum is shown in Figure 2. It is often important to differentiate responses to visible (0.40–0.7 μm), and near-IR (0.7–2.50 μm) radiation.
- Thermal emission spectra at Planck (blackbody) wavelengths in the mid-IR from 2.5 to 35 μm .
- Heating by absorption of atmospheric radiation. Direction-dependent spectra range from 2.5 to 35 μm as shown in Figure 3 for one humidity level [15, 16].
- The photopic response of the human eye and its breakup into blue, green and red color sensitivities [17].

Each of these energy flows is characteristic of a local climate so the best materials may vary accordingly with geography. For clear skies and from directions near the zenith,

the spectral radiance of incoming IR radiation is far from that of a blackbody at atmospheric temperature T_a . It has very low intensity from 7.9 to 13 μm , which we call the “sky window”, as shown in Figure 3 for $T_a = 300$ K, but is blackbody-like in intensity at most other Planck wavelengths, and also at all wavelengths incoming from near the horizon. Thus, we can think of the clear atmosphere as optically equivalent to a surface that combines spectral and angular selectivity. Its spectral properties change from absorption to transmission as it traverses the boundaries of the sky window. These changes may be sharp and large, or weak and low, depending on ray direction to the zenith, and humidity. It is worth noting that at 57° to the zenith one can measure the median incoming IR energy from the whole clear sky [18–20], which is thus very anisotropic in emission intensity.

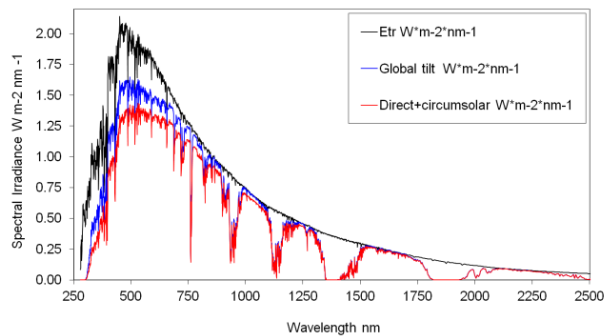


Fig. 2. Solar ASTM G173-03 Reference Spectra [25].

The spectral boundary of most interest, for solar heat collectors or cool roofs and walls, is that between the solar spectrum and the Planck emission spectrum just above and below ambient temperature (10–80°C). It is at 2.5 μm . For best results, both require sharp transitions: absorbers from high absorptance to low emittance, and vice-versa for cool paints. The visible near-IR boundary at 0.7 μm must also be considered for cool paints for two reasons: (a) traditional white pigments such as titanium dioxide (TiO_2) in binder scatter more weakly in the near-IR compared with shorter wavelengths and (b) the binder itself absorbs significantly in the near-IR. Various nanophotonic solutions for higher near-IR reflectance hence higher R_{sol} are possible. If a nonwhite color is included, additional transitions need to be considered with the main aim being the attainment of colored pigment or dyes with limited absorptance in the near-IR. For window and skylight daylighting with low solar heat gain, there are other key boundaries. The main one is again at 0.7 μm , beyond which general

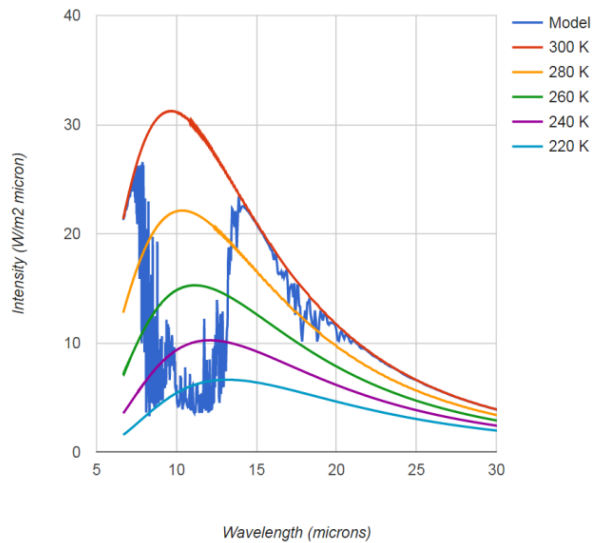


Fig. 3. Downwelling atmospheric infrared spectrum from the zenith, relative to that of a blackbody sky at 300 K. It was calculated using MODTRAN with a clear sky. An appropriately scaled similar modulation occurs for the other blackbody spectra shown [108].

preference is high reflectance to $35\ \mu\text{m}$ for both minimizing solar heat gain and for good insulation. It is sufficient with double and triple glazing to have one internal surface coated. However, glazing systems relying on nanocomposites within polyvinyl butyral (PVB) laminates [21–23] (safety glass) or the particle doping of glass or polymer panels, themselves will switch back at $2.5\ \mu\text{m}$ to high emittance unless at least one additional outer low E surface coating is applied. This layer is ideally a TC, which can be applied postproduction by sputtering or on a float glass production line pyrolytically [24].

A suitable combination of spectrally selective glass and careful heat transfer to maximize convection can produce glass structures that are surprisingly cool even in direct sunlight. The prototypical “NanoHouse” (Figure 4), constructed some years ago in Sydney, Australia, is a case in point. Its interior temperature was acceptable even on a sunny day at 35°C .



Fig. 4. The ‘NanoHouse’, a glass structure designed to demonstrate the best of radiative and convective heat transfer control in a structure exposed to subtropical sunlight (photo, MB Cortie).

3 Modeling material response to the environment

3.1 Nanomaterials in the built environment

This is meant to be a broad ranging descriptive review, so we limit the use of equations in favor of useful references. However, issues in computer predesign deserve a mention

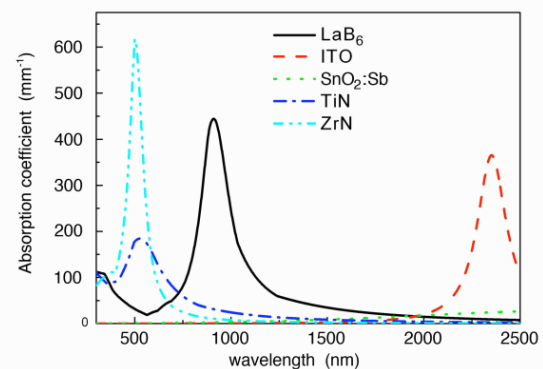


Fig. 5. Resonance plot of various plasmonic nanoparticles in TiO_2 . The different peak locations follow from the changes in carrier densities in each material and the sharpness of each peak depends on carrier relaxation rates. TiN and ZrN do not yield visually clear glazings, while ITO nanoparticles have a resonance, which only weakly impacts on solar transmittance unless the particle loading or fill factor is very much higher than that in LaB_6 , which is ideally located [23].

and some guidance. The demanding spectral and material requirements mean modeling is as indispensable here as it is in architecture itself. Just as architects today must evaluate design options by modeling building performance, optical design results applied to a building component can also be fully evaluated in their application context before they are applied. The development process then becomes efficient. The impact of each of the three environmental spectral systems listed above for any surface plus heat emittance are separately modeled, then their impact combined as appropriate for the energy, lighting and visual impact of each smart nanomaterial.

The standard properties of interest at each wavelength λ , and at angle of incidence θ are: transmittance $T(\lambda, \theta)$, reflectance $R(\lambda, \theta)$ and absorptance $A(\lambda, \theta) = [1 - T(\lambda, \theta) - R(\lambda, \theta)]$. At solar wavelengths, these are weighted with a standard solar spectral density $S(\lambda)$ [25] and integrated. The standard spectra are used for comparing products in large internationally recognized databases, such as the International Glazing Database [26] for window products but have limited use in long-term simulation of a building which needs variable weather data. In Equation (1), solar transmittance at each angle of incidence $T_{\text{sol}}(\theta)$ is calculated. $R_{\text{sol}}(\theta)$ and $A_{\text{sol}}(\theta) = [1 - R_{\text{sol}}(\theta) - T_{\text{sol}}(\theta)]$ result in similar fashion. For the net responses to daylighting, $Y(\lambda)$, the photopic sensitivity of the human eye [17], is first modulated by the solar intensity $S(\lambda)$ to define the incident visible intensity contribution at λ . Integrations as in Equation (2) then yield visible transmittance $T_{\text{vis}}(\theta)$ and reflectance $R_{\text{vis}}(\theta)$.

$$T_{\text{sol}}(\theta) = \int d\lambda T(\lambda, \theta) S(\lambda) / \left(\int d\lambda S(\lambda) \right) \quad (1)$$

$$T_{\text{vis}}(\theta) = \int d\lambda T(\lambda, \theta) S(\lambda) Y(\lambda) / \left(\int d\lambda S(\lambda) Y(\lambda) \right) \quad (2)$$

For artificial light sources, $S(\lambda)$ is replaced in Equation (2) and for x (blue), y (green), z (red), CIE color coordinates $Y(\lambda)$ is replaced by the appropriate color response functions $y(\lambda)$ [17].

These numbers may be sufficient for basic building and fabric simulation and for standardized interproduct comparison, but good model accuracy over extended periods, whether hours, days or a year, needs data or reliable models for the underlying spectral and angular properties. Simple models are often available for $T(\lambda, \theta)$ and $R(\lambda, \theta)$ [27, 28] for common multilayer thin film window coatings, including those using sub-10 nm thick Ag layers. The most efficient approach to this and to simple or extended computational coating design is to start with data or models for the underlying complex refractive indices of

each layer and of the substrate. Final optical properties of a stack of materials follow from these and each layer's thickness [1, 29]. An example of such tuning of the transmittance of a coated window with various thin layers is discussed in Section 5.

3.2 Nanostructure for tunable scattering and optical response

The value in starting with refractive indices is being able to explore fine-tuning of thickness or adjusting of nanostructures to improve solar, visual or thermal performance of a graded or multilayer film before deposition. For nanostructures, suitable effective medium models are useful even if only approximate [30–33]. If scattering is important then single particle modeling can help in design, but multiple scattering is common in smart paints. Thus, approximate approaches such as 4-flux theory [31, 34] and the Kubelka–Munk model [35, 36] are useful as a guide, but other more powerful computational approaches are emerging [37]. Whether a nanocomposite is specular or diffuse, the matrix material must be carefully considered. Its adjustment can be used to improve performance, for example, to downshift plasmonic resonances for better tuning, or to extend strong scattering into the near-IR as is desirable in cool paints. Near-IR absorption peaks for spherical plasmonic nanoparticles embedded in TiO_2 are shown in Figure 5. Changes in carrier density are the main source of these resonance shifts.

3.3 Cooling designs and angular response

The environmental and material parameters governing IR radiant heat flows are important. The downwelling IR spectral intensity at any angle θ to the zenith and wavelength λ under a clear sky depends on the product of atmospheric spectral emittance $E_{\text{atm}}(\text{PWV}, \theta, \lambda)$ and the Planck blackbody emission spectrum $P(\lambda, T_a)$ at atmospheric temperature T_a . Humidity is a very important influence. Its measure here is via precipitable water vapor (PWV), which ranges typically from 3 to 12 mm and is easily linked to dew point or relative humidity. Summing over solid angle and the Planck wavelength range yields the downwelling power $P_{\text{DW}}(T_a, \text{PWV})$ [1]. P_{DW} can range from 200 to 400 W/m^2 [10, 19]. The absorptance of components of this atmospheric radiation by a surface depends on $A_S(\theta, \lambda) = E_S(\theta, \lambda)$ in the range of 2.5–35 μm . The heat removal rate at surface temperature T_s of Equation (4) depends directly on hemispherical emittance $E_{S,H}$

via the integration of $E_S(\theta, \lambda)$ over a hemisphere and the Planck spectrum, with σ the Stefan–Boltzmann constant (of course there is also the question of heat removal by convection to be considered). The rate of heat gain from atmospheric radiation $P_{A,DW}(T_a, PWV)$ is given by Equation (5). The reflected IR is thus $[P_{DW} - P_{A,DW}]$, which adds to the emitted heat to yield the total outflow of IR from the surface. It is worth noting that thermal imaging cameras, which are increasingly being used for checking the performance of IR-smart surfaces, usually sense in a narrow IR band, which happens to largely coincide with wavelengths selectively strongly absorbed in high-quality cool surfaces. What such cameras see outdoors for the best cool surfaces is thus almost entirely thermal emission and little reflectance of IR. Sharp absorption peaks in the sky window zone are thus desirable and can be achieved by well-known dielectric materials in nanoparticle form on metal as we demonstrated in 2010 (Figure 6) [8]. Polymers that absorb selectively in the sky window band are also useful.

$$P_{DW}(T_a, PWV) = \int_0^{\pi/2} d(\sin^2 \theta) \int_0^{\infty} d\lambda P(\lambda, T_a) E_{atm}(\theta, PWV, \lambda) \quad (3)$$

$$P_{S,out}(T_s) = \int_0^{\pi/2} d(\sin^2 \theta) \int_0^{\infty} d\lambda P(\lambda, T_s) E_S(\theta, \lambda) = E_{S,H} \sigma T_s^4 \quad (4)$$

$$P_{A,DW}(T_a, PWV) = \int_0^{\pi/2} d(\sin^2 \theta) \int_0^{\infty} d\lambda P(\lambda, T_a) E_S(\theta, \lambda) E_{atm}(\theta, PWV, \lambda) \quad (5)$$

$E_S(\theta, \lambda)$ of a surface is usually quite distinct from that of the atmosphere $E_{atm}(PWV, \theta, \lambda)$ because of the sky window and the atmosphere's thickness variation with θ . The best way to exploit this difference for a cool roof, wall or fabric varies, and is not well understood. It depends on practical details on how much heat needs to be removed by thermal emission and on the difference between T_a and T_s . The dilemma arises because reducing the heat gain $P_{A,DW}$ in Equation (5) requires reducing $E_S(\theta, \lambda)$ but Equation (4) shows that this also reduces the heat pumping rate. Relevant influences on best choice for $E_S(\theta, \lambda)$ include humidity, building design and structural materials, albedo of coatings, sky fraction in the field-of-view and any other parasitic effects including convective gain or loss from the air. For optimization of cooling rates one thus needs:

- spectral densities of incoming atmospheric radiation and outgoing thermal radiation;
- incident and outgoing IR spectral radiance directional profiles. Both fill the full hemisphere above each surface and depend on humidity. Outgoing IR radiation has two components, thermal emission and reflected IR radiation and
- the desired cooling rate during the day and at night.

As a general rule, unless R_{sol} is above 94% and parasitic heat gain is small, it is preferable to maximize output rate, meaning a high emittance E_S around 0.9 or above is required. This is the case for all “cool” paints available to date. If the sum of solar and other heat gains by our surface is unusually low, say $<60 \text{ W/m}^2$ [10, 38], and if $(T_a - T_s)$ is in the order of $5\text{--}8^\circ\text{C}$, then heat absorbed from the sky ($P_{A,DW}$) will limit achievable cooling. Only then is reduction of $P_{A,DW}$ the best way to maintain net cooling to even lower temperatures. The crossover temperature at which a selective emitter is preferred depends upon heat load, relative surface temperature and environmental conditions [8, 39].

Reduction of $P_{A,DW}$ is done using a high IR reflectance outside the sky window and can be angularly enhanced if incoming rays from the lower sections of the sky are reflected or replaced with those from a low E surface. This latter step exploits the highly directional emittance profile of the sky [1, 15] with $E_{atm}(PWV, \theta, \lambda)$ always close to blackbody values for θ approaching 90° (the horizon). Nanostructures that do this well may be feasible. It is in principle possible to achieve $(T_a - T_s) > 15^\circ\text{C}$ in the daytime and to go lower at night, using special ancillary optics [40, 41]. In all cases, a surface absorptance approaching 1.0 from $7.9\text{--}13 \mu\text{m}$ is always needed, while outside this window, choice of $A(\lambda)$ must be made.

It is important to highlight a common misunderstanding, namely that sky window selective radiative cooling is always preferable to having a near blackbody emitter. Achieving thermal equilibrium with the cold of space sounds attractive, but is rarely practical. If a surface is above ambient temperature most of the daytime, then a high emittance surface is always preferred due to its ability to emit more radiation. It is not until a subambient temperature of more than $\sim 6^\circ\text{C}$ is attained that a crossover to an IR selective coating is preferred as only then is the high E radiative output not enough to overcome the extra gain due to its greater absorption of atmospheric radiation. This is explained in detail in [8] and [39]. An example is enhanced cooling of solar cells utilizing an etched photonic crystal pattern, which needs as high an emittance as possible plus high solar transmittance [42]. This latter

study generated much recent interest. Any gains with such coatings must, however, be referenced to existing photovoltaic (PV) modules in which the radiation from a glass cover already drops cell temperatures by about 5°C relative to a bare wafer. Thus, this complex nanocoating provided just 1.3°C additional cooling for 0.5% more electric power. It is also important to consider open surfaces as convective cooling dominates radiative cooling at typical solar cell temperatures.

Photo-excited carriers in solar cells that thermalize or recombine add to their heat load and directly reduce efficiency. Thus, cooler cells result as internal device efficiency rises from less internal heat generation and also if more solar energy is coupled into the cell. Using micro- and metastructures, both plasmonic and dielectric on silicon yields greater antireflection, more photo-carriers and possibly reduced wafer thickness. This has received much attention over the last decade. A recent extensive review covers the many surface structures that have been examined for this purpose [43]. (Outcoupling of more trapped light from LEDs is also possible using these ideas [44].) Arrays of solar cell modules are increasing their proportion of roof areas either as add-ons or integrated. Thus, they can be considered a growing component of our smart building material inventory, but at current efficiencies the normal operating cell temperatures [45] are much warmer at ~48°C than good cool roofs [46] and thus can add to the urban heat island (UHI) load in cities.

When cloud movement, cloud distribution and humidity changes are included, IR energy flows become statistically very complex. An example is the time series data recently acquired on downwelling IR radiation as shown in Figure 7 [19], which compares IR directionally sensitive data with global IR. Data used for model validation includes exterior surface temperatures, thermal images to examine emitted IR energy, integrated cooling and heating loads and energy use in buildings. Validation with data is important so that designers and architects can have confidence in applying their energy assessment tools to new smart building products in any location.

Finally, a useful aid we found in assessing optical design for use with material spectral data and modeling output is worth mentioning. Collating spectral and angular selectivity for smart outdoor surfaces involves much data. It can, however, be visualized in a single multicolor plot. Doing this greatly aided our recent development of a supercool roof material as shown in Figure 8 for a multi-layer polymer stack with a silver undercoat [10]. The combined response as a function of wavelength from 0.4 to 35 μm across the solar and Planck range and angle of incidence from 0 to 90° is displayed as a false color map of

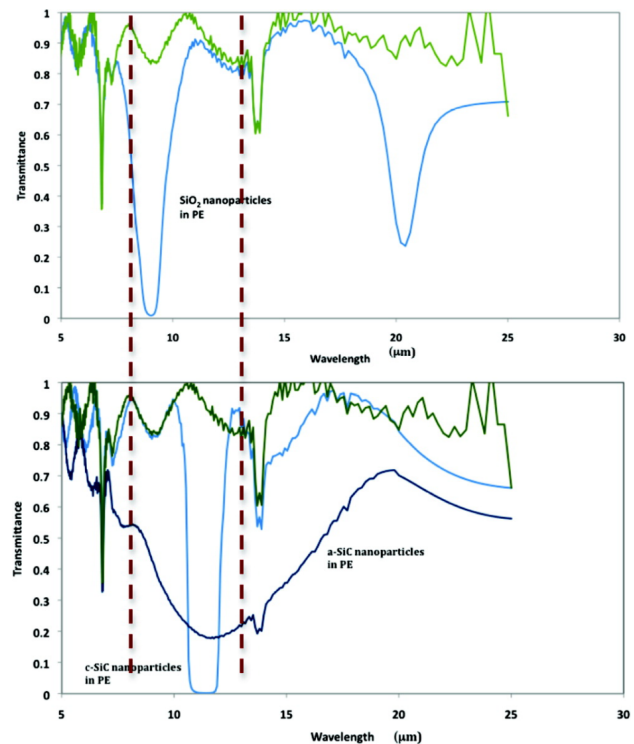


Fig. 6. Transmittance spectra (light blue) of crystalline silica and silicon carbide nanoparticles embedded in polyethylene. These particles resonate at sections of sky window wavelengths where SiO_2 and SiC have negative real permittivity from their phonon responses. Amorphous SiC nanoparticles (dark blue) are only weakly selective as they are much more lossy than their crystalline counterparts. The green plot is for the undoped PE [8].

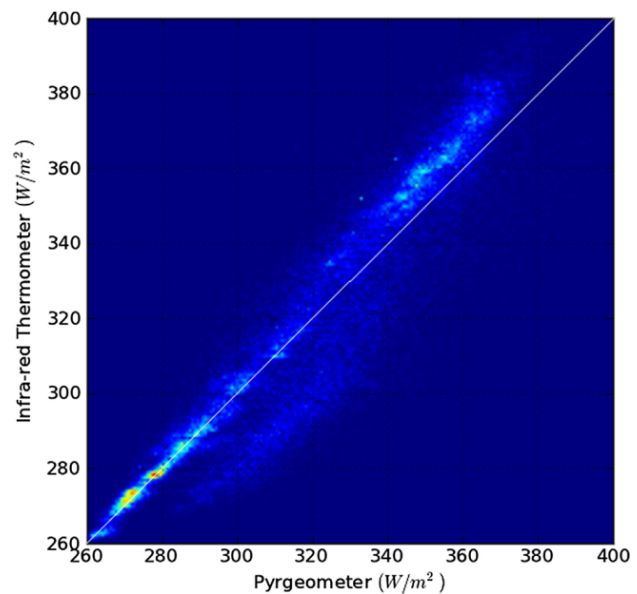


Fig. 7. Atmospheric long-wave downwelling radiation (point-by-point) from an oriented IR thermometer and from a pyrgometer in winter from 9th to 21st of June 2012. The departure from the equality line indicates sky inhomogeneity. The range of intensities is large with major clusters and large spreads.

reflectance or transmittance. The sharpness or otherwise of spectral and angular transitions is easily seen in color boundaries along with constancy across desired bandwidths and angle ranges.

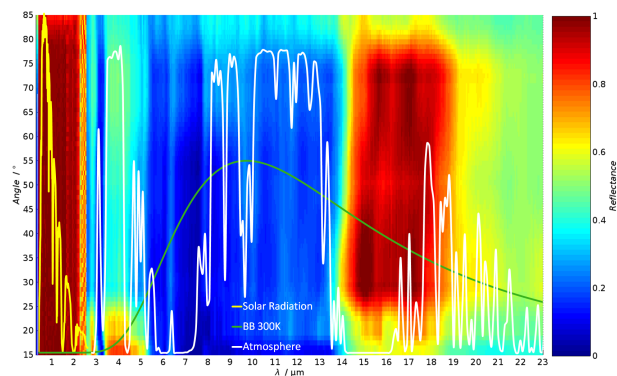


Fig. 8. A two-dimensional plot of supercool roof reflectance in wavelength and angle-of-incidence space. The x-axis spans the solar and blackbody spectral range and the y-axis ray angles to the normal from 0 to 90°. Dark blue is absorptance near 100% dark red reflectance near 100%. The overlays include a plot of the incoming solar spectrum, the emission of a blackbody at 300 K and the atmosphere transparency.

4 Switchable “smart” building materials and fabrics

The word “smart” has two functional aspects: first a human benefit, second the ability to perform electronic and optoelectronic functions such as sensing and power or light generation. All of these can be integrated into buildings and fabrics. Human needs met by smart optical, IR and thermal response of materials is our focus here. Biosensors, or sensors of temperature, solar energy, humidity and light (lux) can be used with our smart materials to force a change in their spectral response, but passive nanophotonic systems can also be “smart” if designed for optimal control of solar heat gain, lumens admitted or to provide cooling or better insulation via control of incoming and outgoing IR radiation. As this brief review will demonstrate, it is amazing how static material surfaces using nanostructures can deal so well with the spectral, geometric, geographic and temporal diversity of incoming radiation.

The word “smart” for light and energy control first came into vogue for chromogenic materials for windows, eyewear and vehicle rear-view mirrors in the 1980s [47–

49]. Photochromics change as a function of incident ultraviolet (UV) intensity, electrochromics in response to applied voltage and thermochromics to temperature change. Li⁺-doped WO₃ dominated electrochromic window studies [50], while pure and doped VO₂ were aimed at thermochromic glazing [50, 51]. Visually acceptable thermochromic results have only recently been indicated by using nanocomposites with Mg-doped VO₂ nanoparticles [52, 53]. This material is so unusual in the structural and electronic (or band structure) components of its insulator-to-metal phase transformations that it is still not well understood (Figure 9). Mixtures of metal and insulator nanophases feature near the transition, and structural and electronic percolation are both involved [54].

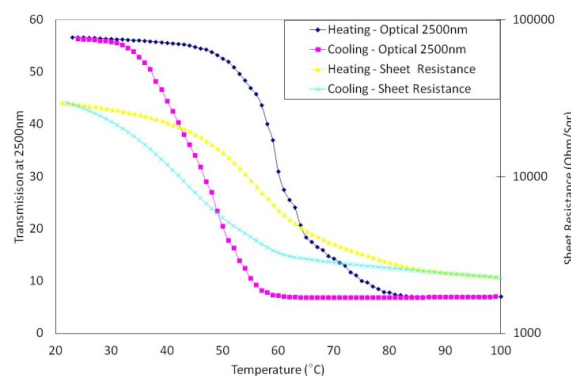


Fig. 9. Typical hysteresis plot of the metal-insulator phase change in VO₂ optical transmission at 2500 nm along with the coincident change in electrical sheet resistance [109].

Though research workers initially focused on energy savings from active window materials, the desire for varying control of glare or lumens admitted turned out to be a higher priority among users [55]. In addition, an appealing visible response was needed for such products to be taken up. For example, basic VO₂ thin films on glass did not lead to commercial thermochromic window products because their visible response was unattractive, and they admitted too few lumens. *That lesson is vital. Smart materials aimed at thermal or lighting control must also be aesthetically attractive if they are to be widely adopted.* Thus, the color and brightness coordinates, and the spatial spread of reflected and transmitted visible range radiation must be included in photonic design. Since IR radiative response is also important, control via material structure and composition over the very broad band from 0.35 to 35 μm is commonly needed. The latter task is simplified if a high emittance works best as with many exterior cool paints.

It is convenient to divide active smart materials into three classes according to how their changing spectral and directional responses arise:

1. *Intrinsic*: Change in properties resulting from a lattice restructure, a phase change or chemical reaction induced in part by changing environmental stimuli. Stimuli of interest include ambient and material temperature changes, and variable intensity of solar irradiation. Well-known responses used are found in windows, polymers or paints using nanoparticles that are thermochromic [53] or photochromic. Fluorescent materials [56] can also respond to solar intensity when used outdoors to maintain contrast in sunlit outdoor signs. Intrinsic photocatalytic or chemical cleaning along with control of incident water drop adherence and flow using nanostructured surfaces can self-clean [57, 58], purify contacting air and collect atmospheric water. Some surfaces mimic nature such as the water collection on a Namibian desert beetle [59]. Self-cleaning process adds durability to desired optical and thermal responses. Nano-TiO₂ [60] and nanofluoropolymers such as polyvinylidene difluoride [61, 62] are already widely used to aid self-cleaning, which is an issue for most surfaces covered in this review including those on fabrics.
2. *Sensor-controlled forcing*: Optical change is induced by applied stimuli such as magnetic and electric fields, applied current or heat, stress and pressure. Variation of angular response to solar radiation, or to alternate between clear or blocked view for privacy is also possible in some composite materials. Phase-change optical shifts can be induced in gasochromic materials [63, 64] including some Mg alloy thin films by introducing hydrogen to form hydrides. Changes in the lattice to store hydrogen lead to associated spectral switching. Electrochromic windows that switch by field-induced intercalation of small ions through nanovoids have been made and applied as shown in Figure 10. Large color or chameleon-like change by stretching nanostructured flexible fabrics has recently been demonstrated [65].
3. *Mixed intrinsic and forced*: A third class of smart dynamic material is emerging. These integrate the generation and storage of electric power needed for forcing change and driving sensors. For example, part of the incident solar energy spectrum on a window might be used to generate electric power to control the remaining spectral and angular response. Mo-

tion and pressure change can also produce power. One day, smart building materials may even harvest photoenergy in chemical form as do plants or algae. Adding separate PV solar cells is not within this category though solar cells are a growing source of power to drive material responses in type (b) switchable materials. Solar fabrics are receiving increased attention, but as yet not for use in direct thermal control.



Fig. 10. An electrochromic window with the left side switched to near-IR and glare blocking mode, and the right side clear. This window was produced by Flabeg and reported by Lampert [47]. Permitted under creative commons license, <http://creativecommons.org/licenses/by-nc-nd/3.0/>

5 Passive nanophotonics in building materials

A range of generic nanostructures are now considered in terms of their ability to provide desired passive solar and IR responses for roofs, walls and windows in a specific location.

5.1 Nanocomposites

These enable both narrow band and broadband tuning of resonant absorption or scattering, and optical anisotropy if needed. Tuning is possible using inclusion size, shape, orientation and arrangement, plus varying the materials used for particles and for the host matrix. Nanovoids form an important inclusions class, though their main use is in achieving a low index medium. Low index layers have many uses. They can strengthen, shift and extend the width of scattering peaks or act as antireflecting outer layer to enhance absorption or transmission in the resonant nanostructures below.

Doping oxides, polymers or polymer layers with noble metal nanoparticles is a common way to achieve sharp plasmonic resonance at visible and, for some shapes, near-IR wavelengths [66–68]. Nevertheless, these are not well suited for use in building windows and skylights for reasons of durability and cost, and because they often reduce light input. In contrast, ceramic ware, colored art glass and some fabrics can use such particles to create interesting decorative color effects and such use extends back to ancient times [69]. Exploitation of plasmonic resonance in particles to block the nonvisible near-IR solar radiation while transmitting light requires conductors with lower plasma frequency than found in Ag and Au. Transparent conducting oxides (TCOs) and certain borides have the required lower carrier densities of order 10^{19} to 10^{21} cm^{-3} . Doping of PVB interlayers in some laminated glass products with indium-tin-oxide (ITO) [57] and lanthanum hexaboride (LaB_6) [18] nanoparticles has resulted in window products, which reduce solar heat gain. Solar absorption by metal-oxide nanocomposites pioneered early advances in spectral selectivity for solar heating with the nanoconductors used such as Cr, C, Mo, Ni and W having broad absorption bands. Low emittance was achieved because the composite film was not thick enough to absorb much IR, so it is strongly reflected by the metal substrate. For most walls and roofs, the spectral response required is the exact opposite to this with low solar absorptance and high emittance. Mixes of complex oxide nanoparticles that absorb for color *just in the visible*, and others such as TiO_2 and zinc oxide (ZnO) that can scatter strongly at all solar wavelengths but absorb beyond $2.5 \mu\text{m}$ to create high emittance when in binder, have an increasing role in achieving this goal. Traditional coloring pigments tend to also absorb in the near-IR.

Colored and clear nano- and microoxide pigments, dye-doped polymer particles and paint binders are being more carefully chosen today. Reducing absorption in the solar near-IR requires nonstandard approaches to paint-

ing. Not only do the older types of colored pigments, fillers and binders absorb too strongly in the near-IR, but the white oxide pigments such as TiO_2 and ZnO, which transmit in this range, are characterized by a Rayleigh scattering strength that falls away in the near-IR. The latter are also unable to mask absorption by the organic binder. Therefore, ways of eliminating or reducing this near-IR fall off in albedo in paints are needed while, simultaneously, the near-IR absorption impact of binder and colored pigments must also be reduced. Optical principles point the way to doing this, but it has to be done without inducing fall off in short wavelength reflectance. The application of nanophotonics has helped and has resulted in new pigments and modified binders involving polyester nanoparticles, which absorb less than acrylic, and in strategies to lower the effective refractive index [70] of the medium in which the TiO_2 or ZnO scatterers are embedded. Better understanding of the impact of the depth profile of composition is another avenue worth further study for modifying spectral and directional response in these complex but ubiquitous particulate systems. The aim is to raise long-term albedo well above 90%. Most cool roofs have much lower average albedos over several years of use, so significant improvement from structural and compositional change driven by new science is expected, despite the long history of paint development.

5.2 Anisotropic nanocomposites for angular and polarization selection

Anisotropy achieved in various ways allows modification of directional-dependent response. Angular selectivity in one layer first received major attention for windows [22, 71] with oblique columnar films, and more recently special stacks of multiple very thin layers [72]. Such metamaterials can be treated as a single effective medium if they do not scatter, although photonic approaches enable additional tunability. These also have strong polarization dependence. This category covers a variety of complex media, including “hyperbolic” dielectrics, which are optically conducting for in-plane polarization and dielectric if the field is normal to the substrate plane.

Columnar materials can be grown over large areas by oblique-incidence physical vapor deposition. Columnar morphology is easily controlled by varying the substrate direction during growth (Figure 11), which in turn controls very strong polarization and angular dependence [14, 73].

Dielectric multilayer stacks built up from very thin oxide or polymer pairs with different indices [10, 74] can provide angular selectivity or flatten response relative to

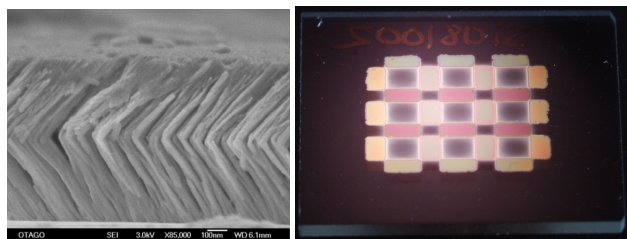


Fig. 11. (Left) An example of tilted anisotropic columns [73], with an abrupt change in orientation achieved through substrate rotation during deposition. (Right) An example of view-angle dependence in columnar films (photo by MD Arnold): the red horizontal rectangles and the olive vertical rectangles have the same optical thickness but different biaxial orientation. This patterning of angular dependence can easily be applied at large and small scales [14].

smooth plane surfaces out to wide angles. Photonic interference effects can also be utilized for sharp angular selectivity [75]. A useful step in adjusting spectral and angular response is for one layer or both in the pair to be anisotropic and also to grade the thickness of the pair across the stack [76]. Coatings of aligned, anisotropic nanoparticles have been shown to have potential too [77], but cost-effective fabrication routes for this type of geometry have yet to be demonstrated.

5.3 Composites using nanoresonance formed from thin oxides on flaky metals

An additional particulate material class is of interest for smart paints and smart fabrics to improve thermal comfort (e.g. maximizing solar reflectance), while providing quality color. The attraction of these is twofold as they also enable tunable and very narrow high-intensity visible absorption bands from a special nanoresonance. This arises when a thin film, typically under 150 nm thick that is partially absorbing, is deposited or grown on a metal or metal film such as stainless steel, nickel, titanium nitride (TiN) and aluminum (Al), which not only reflects, but also partially absorbs [78]. Flakes of metal or dielectric can be used in paints in this way [79, 80]. Al flakes are coated reactively with the absorbing oxide as demonstrated in Figure 12. Examples of this nanoresonance include the many different colors arising from thin spinels on stainless steel [81] or jewelry from anodized titanium.

5.4 Oxide/metal/oxide thin film stacks

Thin film stacks can often behave optically like nanocomposites. They enable tunable sharp spectral or directional

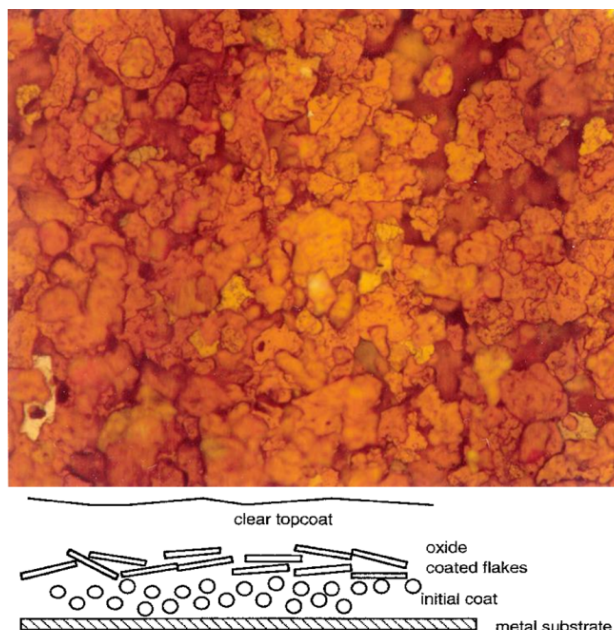


Fig. 12. Optical microscope image from above and cross-section schematic of the profile in a paint layer in which thin oxide-coated Al flakes provide both color and high solar reflectance [80].

transitions at specific wavelengths or angles. Depending on the materials used and the desired spectral outcomes, these can have just one layer or hundreds. The best solar control windows utilize one or more sub-10 nm silver layers between high index oxides, which antireflect the silver for visible solar but not near-IR solar (Figure 14). The Ag layer must be very smooth to avoid localized plasmonic resonant absorption and in addition should be made to grow epitaxially. This allows the Ohmic loss frequency in the Drude response of the ultrathin Ag layer to get very close to the best bulk Ag values of 0.020 eV. For example, on ZnO and Al-doped zinc oxide (AZO), which aid epitaxy, we have made smooth 11 nm thick silver with a Drude loss frequency of just 0.025 eV while on uncoated glass and polymer 20 nm thick Ag layers had loss rates ranging from 0.04 to 0.07 eV. Epitaxy has three practical technical benefits relative to Ag nanolayers on glass, polymers or many other oxides: (i) a much sharper transmittance–reflectance transition from the visible to the near-IR, (ii) a very much lower thermal emittance E for the whole stack and (iii) better flexible options. The three-layer version of this stack such as AZO/Ag/AZO [82] is already of high interest as a flexible TC, being from 70 to 100 nm in total thickness with surface resistivity $<10 \Omega/\text{sq}$ and visible transmittance of 85%. Many active smart building materials including electrochromics, some BPV, organic light-emitting diodes, organic photovoltaics and certain smart fabrics,

can use such stacks. Other advantages over ITO include avoiding the indium supply problem [83] and easier bending.

Metal-insulator stacks with many layer pairs have an emerging role among plasmonic optical materials when precise tuning of spectral and directional response is needed. Multiple colors on a single sample are possible with wedge-shaped nanolayers as shown in Figure 13. Tuning of pass or absorption bandwidth and of transmittance $T(\theta, \varphi)$ is possible [7] by varying the combined thickness of pairs across the stack. Multiple Ag/oxide pairs, TiN/oxide, TiN/nitride and, especially, TiN/AlN pairs are of growing interest for their solar thermal, visual and color responses. As with silver, the quest of late has been for epitaxial nanothin TiN to improve its conductivity and spectral selective switching.

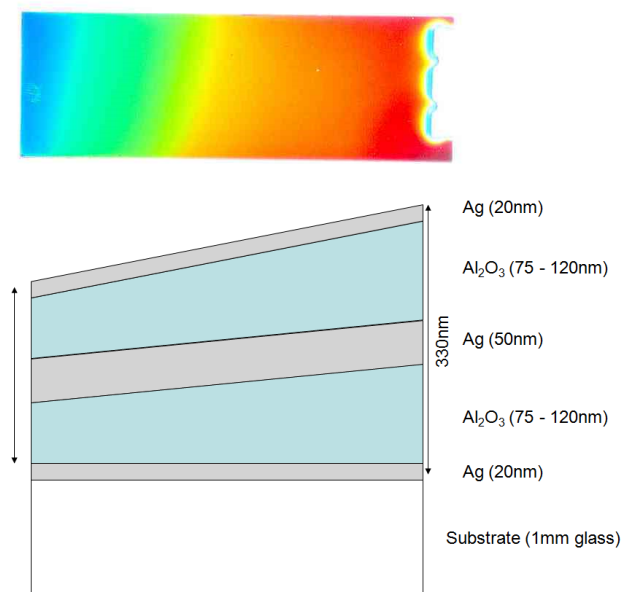


Fig. 13. Example of a wedged oxide/metal/oxide multilayer narrow-band transmission filter. Each point along such a five-layer stack, in which only the dielectrics are graded in thickness, transmits a bright band of light spanning a very small spectral range covering the complete visible spectrum [7].

5.5 All-dielectric spectrally selective absorbers and mirrors

All-dielectric stacks with many nanolayers, sometimes on a metal substrate, have value for everyday functions such as mirrors, cooling and directional control. Our recent benchmark in subambient mid-summer roofing [10] relied

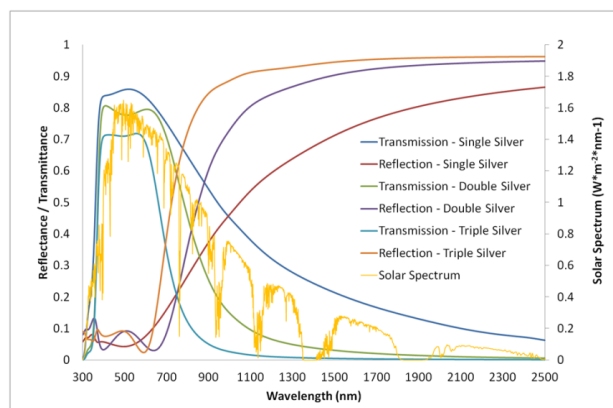


Fig. 14. Spectral reflectance and transmittance of single and multiple (oxide/Ag/oxide) units on glass relative to the solar spectrum. More units have a sharper transition where the eye stops sensing, resulting in higher near-IR reflectance with no major loss of day-lighting capability.

on a stack of 300 pairs of two distinct polyester nanolayers with different refractive indices in which one was isotropic and the second was anisotropic. Both polymers absorbed almost no solar energy. The resulting reflectance was well above 90% across solar wavelengths out to 1.2 μm . A bonus was high IR transmittance where incoming atmospheric thermal radiation dominates, jumping to very high emittance (0.97) across sky window wavelengths. A thin silver layer was added under the polymer sheet to reflect the transmitted solar and IR. A remarkable feature in such stacks is the ability to have almost constant spectral response out to very high angles of incidence (Figure 8). This is achieved by controlled variation of the thickness of each polymer pair from substrate to surface [76]. A similar effect was used in an all-inorganic pair stack used recently to confine transmittance to one incident angle [75]. All-dielectric sputtered stacks of two oxides on silver on silicon have also enabled good cooling [38].

6 Fabrics and wearables

Innovation in the fields of both passive and active smart fabrics has emerged in the last few years as a major new technology trend. The global market for smart fabrics and intelligent textiles and their applications is growing rapidly and is expected to reach around US\$ 2 billion by 2018 [84]. The underpinning basic and applied research has lagged but is growing and nanophotonics expertise is central [85]. Although possibilities are unlimited, here we mention some which can adapt the materials and optical science outlined above for windows, paints and cool

surfaces. While well-established nanoscience underpins much of the activity to date, many fabric- and fiber-specific issues need study, especially for use with natural fibers such as cotton. An example study is binding nanoparticles of ZnO, carbon or nanotubes to natural or synthetic fibers [86]. The convolution of nano-based photonic diversity, with the existing diverse physical and optical world of modern textiles, could grow into a major new special branch of science, technology and materials. Functionalities possible include better and switchable camouflage, thermal control, IR invisibility at thermal camera wavelengths, toxicity to bacteria, electrical conduction, self-cleaning, water shedding and water collecting and removal of harmful gases.

Current fabric capabilities including ability to vary shape for ease of fit, and visual impact must be maintained, while new capabilities in feel and visual design will emerge [87]. Nanofibers just 700 nm in diameter with sufficient strength for combining into a fabric have recently been produced. They are imaged in Figure 15 in an application format. A fabric made from a blend of traditional microfibers and these nanofibers is shown in Figure 16. Textiles woven with many submicron fibers will be ultra-smooth.

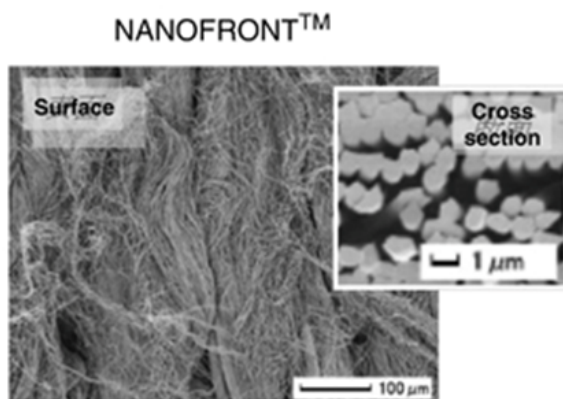


Fig. 15. Nanofiber structures, which can polish and collect dust. Reprinted by permission from Macmillan Publishers Ltd. [87].

Again we limit detailed discussion to passive photonics, though note that much current effort is in *active* photonic textiles such as “solar fabrics” and optoelectronic sensing. The other smart fabric area which parallels some aspects of our roof work [88] is the use in fabrics of phase change materials with transition temperatures between 20

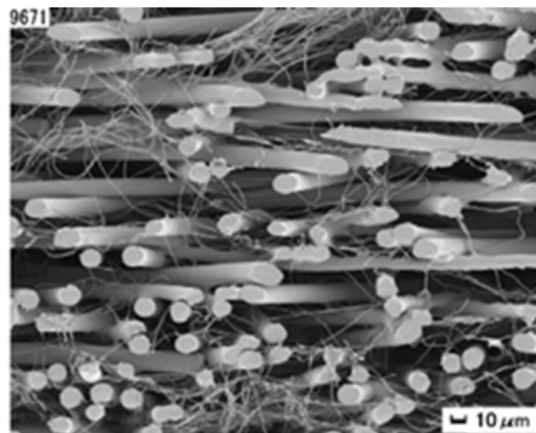


Fig. 16. Cross-section of a fabric made from a 30% blend of 700 nm diameter and standard microfibers. Reprinted by permission from Macmillan Publishers Ltd. [87].

and 28°C. These are also used in some medical and emergency treatment including sterilizing and sensing.

Much work has been done on making fibers and thread conductive for sensing. Conductive metal thread can also be made thermally smart by adding ultrathin nanocoatings as used on colored stainless steel, Al flakes and the mica flakes used in smart paints. Coated metal flakes can also be embedded in thread at the extrusion step. The opposite extreme to one nanolayer on metal flake or film is using hundreds of very thin layer pairs of different index polymers as noted above for our supercool polymer roof. The spectral and angular principles explained above for planar surfaces can apply to threads if suitable polyester pairs are used. Striking colors in dresses [11], as demonstrated in Figure 17, made from the textile product known as Morphotex[®] (a trademark of Teijin Fibers Ltd., Japan) [89, 90], exemplify this approach, but variations in this approach have potential for much more than just novel and compelling appearance.

This “polymer-pair” approach can also be extended to achieve unusual solar thermal IR response in textiles without resorting to using metals. Inspiration can be drawn from our supercool roof coating made with many thickness-graded polyester pairs: an all-polymer multilayer [76, 89] could also be used to make supercool fabrics, which reflect the nonvisible 50% of incident solar energy while retaining color and sky window selective IR properties. These polyester nanosheets and fibers would also produce a strong signal at those wavelengths where thermal imaging camera arrays sense, and could thus be used to help locate people or places as needed at night (e.g.

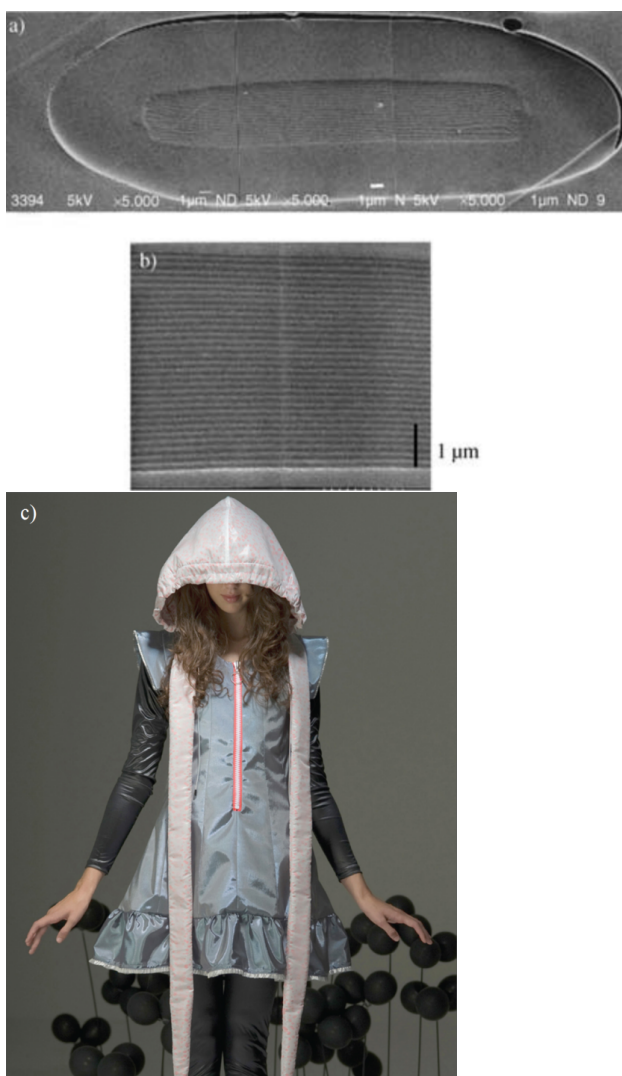


Fig. 17. (A,B) Morphotex cross-sections [83] Image Teijin Fibers Ltd., (C) Morphotex dress (permission from Donna Sgro who is a staff member at the author's university).

by smart sensors on a car or on a special smart phone). Solid objects and fabrics could support such IR contrast. Suitable nanostructured threads could be used to weave numbers, words or names into textiles that would be readable only with IR radiation and sensing. Detection of preset IR contrast by thermal cameras is possible if the background has a lower emittance between 7 and 13 μm . Such polymer multilayer systems will also preserve the color of the underlying thread and dyes while adding solar reflectance. They would be designed to reflect strongly in the near-IR and transmit strongly in the visible (obviously requiring a significant transition in spectral selectivity near 750 nm). The required layer thicknesses can be achieved by drawing fiber from a composite rod (as with Morphotex) with the initial multilayer profile scaled for drawdown.

Predesign must also account for any changes in the polymers anisotropic refractive indices, which are likely after drawing. Such a process led to the Morphotex fabric colors, named as such due to the biomimicry of the Morpho butterfly [89]. For a solar-sensitive switchable fabric it appears feasible to embed thermochromic particles during the extrusion process. Mg-doped VO_2 nanoparticles [52, 53], for retention of visible appeal, or switchable doped VO_2 coatings on fibers or the final textile will preserve underlying thread color while controlling solar heat only when needed.

Such fabrics are more likely initially to be of interest for shading, for example, in outdoor sun umbrellas, decorative collapsible awnings, and beach tents, and in aspects of agriculture and horticulture. For example, low-cost shading solutions to allow good sun for plants while avoiding overheating when solar intensities are too high are also feasible.

TCs which use sub-10 nm layers of Ag are flexible and are hence useful for textiles. They also have low E for retaining heat at night. Visible transparency preserves design colors. Oxide/Ag/oxide stacks can be deposited at low temperature as needed for coating most threads or on a completed textile cloth and have already been demonstrated on thin polyester layers of poly(ethylene terephthalate) and poly(ethylene naphthalate) [82, 91]. Another attraction of such stacks is they can also conduct. A combination of thermal comfort with optoelectronic functionality for wearable solar power sources or sensors is then possible. The TCOs can also be used in nanoparticle form inside a fiber or a polymer layer to absorb near-IR solar radiation if extra daytime heating or reduced transmittance of solar heat is desired. A nanoparticle plasmonic resonance in the near-IR arises if the conducting particle material has a low enough plasma frequency as in ITO or LaB_6 .

Another interesting recent development is the proposal of IR transparent visibly opaque clothing [92], the use of such materials will allow direct radiative cooling of the body for personal thermal management (although the recent decrease in cost of thermal imaging cameras may also raise privacy issues).

7 Mimicking natural nanostructures

The natural world, both living and mineral, contains many nanodesigns, which can be reconstructed or replicated artificially [93–95] to achieve a similar outdoor response to environmental radiation. Many evolved for survival, and

utilized the chemical, thermal and fluidic conditions available in the local environment during particular epochs, so can be improved upon.

Color for camouflage or attracting food based on nanostructure has been widely studied [96]. The grating-like nanostructures in beautiful butterfly wings [90,97] and the inorganic photonic crystals in minerals such as opal can produce very similar bright colors with narrow color spread [98]. Another feature of some natural nanostructures is sharp color shifts with viewing angle, which has already been mimicked in polymeric nanoparticles arrayed into a photonic crystal lattice [99] and ultrathin two-layer coatings on an Al flake [79, 80].

Nano-layering of organic or bio-derived inorganic matter to achieve very high reflectance is well known, for example, in fish scales [100], so predators below cannot distinguish them from the bright sunlight, and in nacre on shells. Many multilayer examples of nonmetallic, very efficient mirrors are finding use in solar energy and building surfaces as featured in this review. The opposite response in some natural nanostructure is the ability to collect incoming scattered light from surroundings very efficiently as in fly eyes [101, 102] including from quite oblique directions. Mimicking such antireflecting nanosurfaces enables enhanced time-averaged transmittance in covers for solar collectors, solar cells and daylighting devices compared with smooth transmitting surfaces, which still reflect strongly at oblique incidence. Structural hierarchies with microstructures overlaid with nanostructures can be used in windows and skylights to minimize transmitted glare [103].

Natural structures also help cool in sunlight. Desert silver ants have relatively high solar reflecting backs so they can find food in the fierce daytime heat to avoid night predators [104]. A most important example is leaves. While they cool in part by evapotranspiration, their water content would still raise temperatures too high for survival if the ~50% of solar energy in the near-IR was significantly absorbed. To avoid this, leaves evolved large empty pores enclosed within thin membranes in their waxy zones so the overall structure scatters near-IR radiation strongly [31]. Some high solar reflecting paints have adopted a similar strategy by adding hollow core inorganic particles to minimize the near-IR absorption of paint binders [105].

8 Conclusion

This short review has outlined the material, optical and environmental principles that have enabled passive and active smart building materials, such as paints, glazings and fabrics, to be modeled and then made. The majority of applications considered involved surfaces exposed to the sun, the night sky and atmospheric gases. Optimized spectral and angular selectivity at visible, solar and thermal wavelengths often requires sharp transitions at particular wavelengths governed by the spectra of solar and atmospheric radiation plus our vision, thermal comfort and aesthetic needs. Control across such a wide-band of wavelengths commonly requires a hierarchy of nanostructures. Smart fabrics can utilize the same nanophotonic principles adapted to the production and modification of thread, fibers and complete textiles. Switchable options or chromogenics were also considered, including the use of thermally induced phase change in films and particles. The impact of “switchables” in building technology has not as yet lived up to the initial promise for a variety of reasons; however, their exciting and lower cost offers prospects in the area of smart wearables. Eyewear with UV-induced transmittance switching is to date the greatest direct human impact of switchable optics. It is possible that our clothing and agricultural fabrics may prove to be the catalyst for a second switchable age. If this is to occur then switchables involving nanophotonics will be needed.

These technologies are not just aimed at energy saving and direct offsets of CO₂ emissions [1, 106, 107]. They can improve the local outdoor environment, and the complete human experience. Health, medical and psychological benefits result. Consider the multiple benefits of nanophotonic spectral control in the latest coatings available for cool roofing as a concluding example: these save energy, reduce peak power problems in summer and, if widely used, could even mediate the UHI problem in cities.

Acknowledgment: Donna Sgro from our Faculty of Design, Architecture and Building, designed and produced the smart dresses made from Morphotex nanofibers while in Japan, and permitted us to use one of her many images. The authors' contributions to aspects of the work covered within this review since 2010 has been supported in part by two Australian Research Council Discovery grants DP0987354 and DP140102003.

References

- [1] G. B. Smith, and C. G. Granqvist, *Green nanotechnology: solutions for sustainability and energy in the built environment*, CRC Press 2010.
- [2] US Department of Energy, EnergyPlus Energy Simulation Software, 2015
- [3] NFRC, "ANSI/NFRC 200-2014 Procedure for determining fenestration product solar heat gain coefficient and visible transmittance at normal incidence," 2014.
- [4] M. Sleiman, G. Ban-Weiss, H. E. Gilbert et al., "Soiling of building envelope surfaces and its effect on solar reflectance—Part I: Analysis of roofing product databases," *Solar Energy Materials and Solar Cells* **95**(12), 3385-3399, <http://dx.doi.org/10.1016/j.solmat.2011.08.002>, 2011.
- [5] P. J. Brown, and K. Stevens, *Nanofibers and nanotechnology in textiles*, Woodhead Publishing 2007.
- [6] M. Teodorescu, "Applied Biomimetics: A New Fresh Look of Textiles," *Journal of Textiles* **9**, doi:10.1155/2014/154184, 2014.
- [7] A. Gentle, and G. Smith, "Five layer narrow band position variable filters for sharp colours and ultra low emittance," *Applied Physics B* **92**(1), 67-72, 2008.
- [8] A. R. Gentle, and G. B. Smith, "Radiative heat pumping from the earth using surface phonon resonant nanoparticles," *Nano letters* **10**(2), 373-379, 2010.
- [9] SOLASOLV® Aviation system sun screens - sun protection for air traffic control towers, 2015. (Accessed 03/09/15 at <http://www.solasolv.com/air-traffic-control-tower-sunscreen.php>)
- [10] A. R. Gentle, and G. B. Smith, "A subambient open roof surface under the mid-summer sun," *Advanced Science* **2**(9), doi:<http://dx.doi.org/10.1002/adv.201500119>, 2015.
- [11] S. Meng, "Donna Sgro: the Teijin fibers," in *Think Magazine*, pp. 35-40 2011.
- [12] N. Pan, "Exploring the significance of structural hierarchy in material systems—A review," *Applied Physics Reviews* **1**(2), 021302, doi:<http://dx.doi.org/10.1063/1.4871365>, 2014. (
- [13] P. Ščajev, T. Malinauskas, G. Seniutinas et al., "Light-induced reflectivity transients in black-Si nanoneedles," *Solar Energy Materials and Solar Cells* **144**(221-227, <http://dx.doi.org/10.1016/j.solmat.2015.08.030>, 2016.
- [14] M. Arnold, I. Hodgkinson, Q. Wu, and R. Blaikie, "Multi-axis retarder arrays by masked oblique deposition," *Journal of Vacuum Science & Technology B* **23**(4), 1398-1404, 2005.
- [15] P. Berdahl, and R. Fromberg, "The thermal radiance of clear skies," *Solar Energy* **29**(4), 299-314, 1982.
- [16] C. Granqvist, and A. Hjortsberg, "Radiative cooling to low temperatures: general considerations and application to selectively emitting SiO films," *Journal of Applied Physics* **52**(6), 4205-4220, 1981.
- [17] G. Wyszecki, and W. S. Stiles, *Color science: concepts and methods, quantitative data and formulae*, Wiley 2000.
- [18] W. H. Dines, *Monthly mean values of radiation from various parts of the sky at Benson, Oxfordshire*, Edward Stanford 1927.
- [19] J. L. Castro Aguilar, A. R. Gentle, G. B. Smith, and D. Chen, "A method to measure total atmospheric long-wave down-welling radiation using a low cost infrared thermometer tilted to the vertical," *Energy* **81**, 233-244, doi:10.1016/j.energy.2014.12.035, 2015.
- [20] S. Sakai, A. Ito, K. Umetani, I. Iizawa, and M. Onishi, "A practical pyrometer using the representative angle," *Journal of Atmospheric and Oceanic Technology* **26**(3), 647-655, doi:10.1175/2008JTECHA1076.1, 2009.
- [21] S. Schelm, and G. B. Smith, "Dilute LaB6 nanoparticles in polymer as optimized clear solar control glazing," *Applied Physics Letters* **82**(24), 4346-4348, doi:10.1063/1.1584092, 2003.
- [22] G. B. Smith, S. Dligatch, R. Sullivan, and M. G. Hutchins, "Thin film angular selective glazing," *Solar Energy* **62**(3), 229-244, doi:10.1016/S0038-092X(98)00009-7, 1998.
- [23] S. Schelm, G. B. Smith, P. D. Garrett, and W. K. Fisher, "Tuning the surface-plasmon resonance in nanoparticles for glazing applications," *Journal of Applied Physics* **97**(12), 124314, doi:10.1063/1.1924873, 2005.
- [24] Pilkington K Glass, Pilkington, 2015. (Accessed 1/09/2015 at <https://www.pilkington.com/en-gb/uk/products/product-categories/thermal-insulation/pilkington-k-glass-range/pilkington-k-glass>)
- [25] ASTM, "G173 - 03 Standard tables for reference solar spectral irradiances: direct normal and hemispherical on 37°tilted surface," 2012.
- [26] Lawrence Berkeley National Laboratory, The International Glazing Database (IGDB), <http://windowoptics.lbl.gov/data/igdb>, 2015
- [27] A. Roos, P. Polato, P. A. Van Nijnatten, M. G. Hutchins, F. Olive, and C. Anderson, "Angular-dependent optical properties of low-e and solar control windows—: Simulations versus measurements," *Solar Energy* **69**, 15-26, 2001.
- [28] Lawrence Berkeley National Laboratory, Window, <https://windows.lbl.gov/software/window/window.html>, 2015.
- [29] WVASE - Ellipsometry analysis software, J.A. Woollam Co., 2015. (Accessed at <http://www.jawoollam.com/WVASE.html>)
- [30] D. A. G. Bruggeman, "Berechnung verschiedener physikalischer Konstanten von heterogenen Substanzen," *Ann. Phys. (Leipzig)* **24**(636-679), 1935.
- [31] S. Jacquemoud, and L. Ustin, "Modeling leaf optical properties," *Photobiological Sciences Online* 2008.
- [32] J. C. Maxwell Garnett, "Colours in metal glasses and in metallic films," *Royal Society of London Philosophical Transactions Series A* **385-420**, 1904.
- [33] A. Lakhtakia, *Selected papers on linear optical composite materials*, Society of Photo Optical Engineers 1996.
- [34] W. E. Vargas, and G. A. Niklasson, "Forward average path-length parameter in four-flux radiative transfer models," *Applied Optics* **36**(16), 3735-3738, doi:10.1364/AO.36.003735, 1997.
- [35] P. Kubelka, F. Munk, and P. Kubelka, "Ein Beitrag zur Optik der Farbanstriche," *Zeitschrift für technische Physik* **12**, 593-501, 1931.
- [36] English Translation of Ein Beitrag zur Optik der Farbanstriche - An Article on Optics of Paint Layers, S. H. Westin, 2004. (Accessed 4/9/2015 at <http://www.graphics.cornell.edu/~westin/pubs/kubelka.pdf>)
- [37] B. T. Draine, and P. J. Flatau, "Discrete-dipole approximation for scattering calculations," *J. Opt. Soc. Am. A* **11**(4), 1491-1499, doi:10.1364/JOSAA.11.001491, 1994.
- [38] A. P. Raman, M. A. Anoma, L. Zhu, E. Rephaeli, and S. Fan, "Passive radiative cooling below ambient air tempera-

- ture under direct sunlight," *Nature* **515**(7528), 540-544, doi:10.1038/nature13883, 2014.
- [39] A. Gentle, and G. Smith, "Performance comparisons of sky window spectral selective and high emittance radiant cooling systems under varying atmospheric conditions," *Proceedings Solar2010, The 48th AuSES Annual Conference* 2010.
- [40] G. Smith, "Amplified radiative cooling via optimised combinations of aperture geometry and spectral emittance profiles of surfaces and the atmosphere," *Solar Energy Materials and Solar Cells* **93**(9), 1696-1701, 2009.
- [41] F. Trombe, "Perspectives sur l'utilisation des rayonnements solaires et terrestres dans certaines régions du monde," *Rev. Gen. Therm* **6**(70), 1285, 1967.
- [42] L. Zhu, A. P. Raman, and S. Fan, "Radiative cooling of solar absorbers using a visibly transparent photonic crystal thermal blackbody," *Proceedings of the National Academy of Sciences* **112**(40), 12282-12287, 10.1073/pnas.1509453112, 2015.
- [43] M. L. Brongersma, Y. Cui, and S. Fan, "Light management for photovoltaics using high-index nanostructures," *Nat Mater* **13**(5), 451-460, 10.1038/nmat3921, 2014.
- [44] S. Pillai, K. R. Catchpole, T. Trupke, G. Zhang, J. Zhao, and M. A. Green, "Enhanced emission from Si-based light-emitting diodes using surface plasmons," *Applied Physics Letters* **88**(16), 161102, doi:http://dx.doi.org/10.1063/1.2195695, 2006.
- [45] R. G. Ross, "Flat-plate photovoltaic array design optimization," in *14th IEEE Photovoltaic Specialists Conference*, San Diego, CA 1980.
- [46] H. Akbari, and R. Levinson, "Evolution of cool-roof standards in the US," *Advances in building energy research* **2**(1), 1-32, 2008.
- [47] C. M. Lampert, "Chromogenic smart materials," *Materials today* **7**(3), 28-35, 2004.
- [48] C. Granqvist, "Chromogenic materials for transmittance control of large-area windows," *Critical Reviews in Solid State and Material Sciences* **16**(5), 291-308, 1990.
- [49] J. Svensson, and C. Granqvist, "Electrochromic coatings for "smart windows", " *Solar energy materials* **12**(6), 391-402, 1985.
- [50] G. A. Niklasson, and C. G. Granqvist, "Electrochromics for smart windows: thin films of tungsten oxide and nickel oxide, and devices based on these," *Journal of Materials Chemistry* **17**(2), 127-156, 2007.
- [51] A. R. Gentle, G. B. Smith, and A. I. Maarof, "Frequency and percolation dependence of the observed phase transition in nanostructured and doped VO₂ thin films," *Journal of Nanophotonics* **3**(1), 031505-031505-031515, 2009.
- [52] N. Mlyuka, G. Niklasson, and C.-G. Granqvist, "Mg doping of thermochromic VO₂ films enhances the optical transmittance and decreases the metal-insulator transition temperature," *Applied physics letters* **95**(17), 171909, 2009.
- [53] S.-Y. Li, N. R. Mlyuka, D. Primetzhofner et al., "Bandgap widening in thermochromic Mg-doped VO₂ thin films: quantitative data based on optical absorption," *Applied Physics Letters* **103**(16), 161907, 2013.
- [54] M. M. Qazilbash, M. Brehm, B.-G. Chae et al., "Mott transition in VO₂ revealed by infrared spectroscopy and nano-imaging," *Science* **318**(5857), 1750-1753, 2007.
- [55] E. S. Lee, and D. DiBartolomeo, "Application issues for large-area electrochromic windows in commercial buildings," *Solar Energy Materials and Solar Cells* **71**(4), 465-491, 2002.
- [56] W. Wiemer, and A. Bohm, Liquid Crystal Display Device patent US20080074575. 2008.
- [57] L. Österlund, "Structure-reactivity relationships of anatase and rutile TiO₂ nanocrystals measured by in situ vibrational spectroscopy," *Solid State Phenomena* 203-219 (2010).
- [58] Pilkington self-cleaning glass: technical FAQs, Pilkington, 2015. (Accessed 04/09/2015 at <https://www.pilkington.com/en-gb/uk/householders/types-of-glass/self-cleaning-glass/faqs/technical-faqs>)
- [59] A. R. Parker, and C. R. Lawrence, "[Water capture by a desert beetle](#)," *Nature* **414**(6859), 33-34, doi:10.1038/35102108, 2001.
- [60] E. I. Cedillo-González, R. Riccñ, M. Montorsi, M. Montorsi, P. Falcaro, and C. Siligardi, "Self-cleaning glass prepared from a commercial TiO₂ nano-dispersion and its photocatalytic performance under common anthropogenic and atmospheric factors," *Building and Environment* **71**, 7-14, doi:10.1016/j.buildenv.2013.09.007, 2014.
- [61] Z. Zheng, Z. Gu, R. Huo, and Z. Luo, "Fabrication of self-cleaning poly(vinylidene fluoride) membrane with micro/nanoscaled two-tier roughness," *Journal of Applied Polymer Science* **122**(2), 1268-1274, doi:10.1002/app.34254, 2011.
- [62] R. A. Iezzi, S. Gaboury, and K. Wood, "Acrylic-fluoropolymer mixtures and their use in coatings," *Progress in organic coatings* **40**(1), 55-60, 2000.
- [63] D. Schweiger, A. Georg, W. Graf, and V. Wittwer, "Examination of the kinetics and performance of a catalytically switching (gasochromic) device," *Solar Energy Materials and Solar Cells* **54**(1), 99-108, 1998.
- [64] J.-L. Chen, C.-C. Chang, Y.-K. Ho et al., "Behind the color switching in gasochromic VO₂," *Physical Chemistry Chemical Physics* **17**(5), 3482-3489, doi:10.1039/C4CP04623D, 2015.
- [65] L. Zhu, J. Kapraun, J. Ferrara, and C. J. Chang-Hasnain, "Flexible photonic metastructures for tunable coloration," *Optica* **2**(3), 255-258, doi:10.1364/OPTICA.2.000255, 2015.
- [66] N. L. Stokes, J. A. Edgar, A. M. McDonagh, and M. B. Cortie, "[Spectrally selective coatings of gold nanorods on architectural glass](#)," *Journal of Nanoparticle Research* **12**(8), 2821-2830, 2010.
- [67] X. Xu, T. Gibbons, and M. Cortie, "[Spectrally-selective gold nanorod coatings for window glass](#)," *Gold Bulletin* **39**(4), 156-165, 2006.
- [68] M. Faraday, "The Bakerian Lecture: Experimental Relations of Gold (and Other Metals) to Light," *Philosophical Transactions of the Royal Society of London* **147**, 145-181, doi:10.2307/108616, 1857.
- [69] I. Freestone, N. Meeks, M. Sax, and C. Higgitt, "The Lycurgus cup—a Roman nanotechnology," *Gold Bulletin* **40**(4), 270-277, 2007.
- [70] R. Iezzi, "Creating coatings for better buildings," *Paint Coat. Ind. (July 1998)* **48**, 60, 1998.
- [71] G. Mbise, G. B. Smith, G. A. Niklasson, and C. G. Granqvist, "Angular-selective optical properties of Cr films made by oblique-angle evaporation," *Applied Physics Letters* **54**(11), 987-989, doi:10.1063/1.100757, 1989.

- [72] T. Xu, and H. J. Lezec, "Visible-frequency asymmetric transmission devices incorporating a hyperbolic metamaterial," *Nat Commun* **5**, doi:10.1038/ncomms5141, 2014.
- [73] I. Hodgkinson, L. De Silva, and M. Arnold, "Inorganic polarizing materials grown by physical vapor deposition," *Proc. SPIE 5870, Advances in Thin-Film Coatings for Optical Applications II*, 587001-587015, doi:10.1117/12.613990, 2005.
- [74] M. F. Weber, C. A. Stover, L. R. Gilbert, T. J. Nevitt, and A. J. Ouderkirk, "Giant Birefringent Optics in Multilayer Polymer Mirrors," *Science* **287**(5462), 2451-2456, doi:10.1126/science.287.5462.2451, 2000.
- [75] Y. Shen, D. Ye, I. Celanovic, S. G. Johnson, J. D. Joannopoulos, and M. Soljačić, "Optical Broadband Angular Selectivity," *Science* **343**(6178), 1499-1501, doi:10.1126/science.1249799, 2014.
- [76] L. Gilbert, M. F. Weber, R. J. Strharsky, C. A. Stover, T. J. Nevitt, and A. J. Ouderkirk, "Giant birefringent optics in multilayer polymer filters," in OSA Technical Digest Series, *Optical Interference Coatings FA2* (2001).
- [77] J. Liu, B. Cankurtaran, L. Wiczorek, M. J. Ford, and M. Cortie, "Anisotropic optical properties of semitransparent coatings of gold nanocaps," *Advanced Functional Materials* **16**(11), 1457-1461, 2006.
- [78] M. A. Kats, R. Blanchard, P. Genevet, and F. Capasso, "Nanometre optical coatings based on strong interference effects in highly absorbing media," *Nature materials* **12**(1), 20-24, 2013.
- [79] G. B. Smith, A. Gentle, P. Swift, A. Earp, and N. Mronga, "Coloured paints based on coated flakes of metal as the pigment, for enhanced solar reflectance and cooler interiors: description and theory," *Solar Energy Materials and Solar Cells* **79**(2), 163-177, doi:10.1016/S0927-0248(02)00409-9, 2003.
- [80] G. B. Smith, A. Gentle, P. D. Swift, A. Earp, and N. Mronga, "Coloured paints based on iron oxide and silicon oxide coated flakes of aluminium as the pigment, for energy efficient paint: optical and thermal experiments," *Solar Energy Materials and Solar Cells* **79**(2), 179-197, doi:10.1016/S0927-0248(02)00410-5, 2003.
- [81] T. Evans, A. Hart, and A. Skedgell, "Nature of the film on coloured stainless steel," *Trans. Inst. Metal Finishing, Summer 1973*, **51**, (3), 108-112 1973.
- [82] A. R. Gentle, S. D. Yambem, G. B. Smith, P. L. Burn, and P. Meredith, "Optimized multilayer indium-free electrodes for organic photovoltaics," *physica status solidi (a)* **212**(2), 348-355, 2015.
- [83] T. Minami, "Present status of transparent conducting oxide thin-film development for Indium-Tin-Oxide (ITO) substitutes," *Thin Solid Films* **516**(17), 5822-5828, <http://dx.doi.org/10.1016/j.tsf.2007.10.063>, 2008.
- [84] Global smart, intelligent, digital & interactive fabrics/textile market revenue from 2012 to 2018 (in billion U.S. dollars)*, Statista, 2015. (Accessed 04/09/2015 at <http://www.statista.com/statistics/302526/smart-fabrics-market-revenue-worldwide/>)
- [85] Innovation in Textiles - Cornell University uses nanotech to transform cotton fibres, B. Hunter, 2015. (Accessed 04/09/2015 at <http://www.innovationintextiles.com/smart-textiles-nanotechnology/cornell-university-uses-nanotech-to-transform-cotton-fibres/>)
- [86] S. Ovalle-Serrano, V. Carrillo, C. Blanco-Tirado, J. Hinestroza, and M. Combariza, "Controlled synthesis of ZnO particles on the surface of natural cellulosic fibers: effect of concentration, heating and sonication," *Cellulose* **22**(3), 1841-1852, 2015.
- [87] M. Kamiyama, T. Soeda, S. Nagajima, and K. Tanaka, "Development and application of high-strength polyester nanofibers," *Polym J* **44**(10), 987-994, 2012.
- [88] J. L. C. Aguilar, G. B. Smith, A. R. Gentle, and D. Chen, "Optimum integration of albedo, sub-roof R-value, and phase change material for cool roofs," *Proceedings of Building Simulation 2013: 13th Conference of the International Building Performance Simulation Association. Chambéry (France), 25-28 August 2013* (2013).
- [89] M. I. E. Yoshimura, K. Iohara, H. Tabata, and S. Shimizu, "Structurally Colored Fibers "MORPHOTEX"," *Sen'i Gakkaishi* **56**(12), 348-351, doi:10.2115/fiber.56.P_348, 2000.
- [90] S. Kinoshita, and S. Yoshioka, "Structural Colors in Nature: The Role of Regularity and Irregularity in the Structure," *ChemPhysChem* **6**(8), 1442-1459, doi:10.1002/cphc.200500007, 2005.
- [91] S. D. Yambem, M. Ullah, K. Tandy, P. L. Burn, and E. B. Namdas, "ITO-free top emitting organic light emitting diodes with enhanced light out-coupling," *Laser & Photonics Reviews* **8**(1), 165-171, 2014.
- [92] J. K. Tong, X. Huang, S. V. Boriskina, J. Loomis, Y. Xu, and G. Chen, "Infrared-transparent visible-opaque fabrics for wearable personal thermal management," *ACS Photonics* **2**(6), 769-778, 10.1021/acsphotonics.5b00140, 2015.
- [93] T. Starkey, and P. Vukusic, "Light manipulation principles in biological photonic systems," *Nanophotonics* **2**(4), 289-307, 2013.
- [94] D. P. Pulsifer, and A. Lakhtakia, "Background and survey of bioreplication techniques," *Bioinspiration & biomimetics* **6**(3), 031001, 2011.
- [95] K. Liu, and L. Jiang, "Multifunctional integration: from biological to bio-inspired materials," *ACS Nano* **5**(9), 6786-6790, 10.1021/nn203250y, 2011.
- [96] A. R. Parker, "515 million years of structural colour," *Journal of Optics A: Pure and Applied Optics* **2**(6), R15-R28, 2000.
- [97] H. Ghiradella, "Light and color on the wing: structural colors in butterflies and moths," *Applied Optics* **30**(24), 3492-3500, 1991.
- [98] C. I. Aguirre, E. Reguera, and A. Stein, "Tunable colors in opals and inverse opal photonic crystals," *Advanced Functional Materials* **20**(16), 2565-2578, 2010.
- [99] M. Boyle, A. Neumeister, R. Kiyan et al., "Production of 3D photonic components with ultrafast micromachining," 646212-646212-646219 (2007).
- [100] N. Shashar, R. Hagan, J. G. Boal, and R. T. Hanlon, "Cuttlefish use polarization sensitivity in predation on silvery fish," *Vision Research* **40**(1), 71-75, [http://dx.doi.org/10.1016/S0042-6989\(99\)00158-3](http://dx.doi.org/10.1016/S0042-6989(99)00158-3), 2000.
- [101] A. R. Parker, Z. Hegedus, and R. A. Watts, "Solar-absorber antireflector on the eye of an Eocene fly (45 Ma)," *Proceedings of the Royal Society of London B: Biological Sciences* **265**(1398), 811-815, 10.1098/rspb.1998.0364, 1998.
- [102] A. Gombert, W. Glaubitt, K. Rose et al., "Subwavelength-structured antireflective surfaces on glass," *Thin Solid Films* **351**(1), 73-78, 1999.

- [103] A. Gombert, B. Bläsi, C. Bu, P. Nitz, W. Hoßfeld, and M. Niggemann, "Some application cases and related manufacturing techniques for optically functional microstructures on large areas," *Optical Engineering* **43**(11), 2525-2533, 2004.
- [104] N. N. Shi, C.-C. Tsai, F. Camino, G. D. Bernard, N. Yu, and R. Wehner, "Keeping cool: enhanced optical reflection and radiative heat dissipation in Saharan silver ants," *Science* **349**(6245), 298-301, 2015.
- [105] I. Mussard, "25 Years of hollow-sphere hiding technology," *Paint & Coatings Industry* **21**(9), 96, 2005.
- [106] I. Edmonds, and G. Smith, "Surface reflectance and conversion efficiency dependence of technologies for mitigating global warming." *Renewable Energy* **36**(5), 1343-1351, 2011.
- [107] H. Akbari, S. Menon, and A. Rosenfeld, "Global cooling: increasing world-wide urban albedos to offset CO₂," *Climatic Change* **94**(3-4), 275-286, 2009.
- [108] MODTRAN Infrared Light in the Atmosphere, 2015. (Accessed 04/09/2015 at <http://climatemodels.uchicago.edu/modtran/>)
- [109] A. R. Gentle, A. I. Maarooof, M. B. Cortie, and G. B. Smith, "Optical and electrical switching in nanostructured coatings of VO₂," *NanoScience+ Engineering* 664709-664709-664708 (2007).